frontiers | Frontiers in Earth Science

TYPE Original Research
PUBLISHED 17 April 2024
DOI 10.3389/feart.2024.1383146

OPEN ACCESS

EDITED BY
Julie Lattaud,
University of Basel, Switzerland

REVIEWED BY
Céline Martin,
Binghamton University, United States
Fatemeh Ajallooeian,
ETH Zürich, Switzerland

*CORRESPONDENCE
Sergio Contreras,
scontreras@ucsc.cl
Josef P. Werne,
jwerne@pitt.edu

RECEIVED 06 February 2024
ACCEPTED 05 April 2024
PUBLISHED 17 April 2024

CITATION
O'Beirne MD, Scott WP, Contreras S, Araneda A, Tejos E, Moscoso J and Werne JP (2024), Distribution of branched glycerol dialkyl glycerol tetraether (brGDGT) lipids from soils and sediments from the same watershed are distinct regionally (central Chile) but not globally.
Front. Earth Sci. 12:1383146.
doi: 10.3389/feart.2024.1383146

Distribution of branched glycerol dialkyl glycerol tetraether (brGDGT) lipids from soils and sediments from the same watershed are distinct regionally (central Chile) but not globally

Molly D. O'Beirne[1], Wesley P. Scott[1], Sergio Contreras[1,2,3]*, A. Araneda[4], E. Tejos[2], J. Moscoso[5] and Josef P. Werne[1]*

[1]Department of Geology and Environmental Science, University of Pittsburgh, Pittsburgh, PA, United States, [2]Departamento de Química Ambiental, Universidad Católica de la Santísima Concepción, Concepción, Chile, [3]Centro de Investigación en Biodiversidad y Ambientes Sustentables (CIBAS), Concepción, Chile, [4]Departamento de Sistemas Acuáticos, Facultad de Ciencias Ambientales y Centro EULA-Chile, Universidad de Concepción, Concepción, Chile, [5]Ecogestión Ambiental Ltda., Chiguayante, Chile

Quantitative reconstructions of past continental climates are vital for understanding contemporary and past climate change. Branched glycerol dialkyl glycerol tetraethers (brGDGTs) are unique bacterial lipids that have been proposed as universal paleothermometers due to their correlation with temperature in modern settings. Thus, brGDGTs may serve as a crucial paleotemperature proxy for understanding past climate variations and improving regional climate projections, especially in critical but under constrained regions. That said, complications can arise in their application due to varying source contributions (e.g., soils vs. peats vs. lacustrine). As such, this study investigates brGDGT distributions in Chilean lake surface sediments and corresponding watershed soils to determine the source of brGDGTs to lake sediments. Global datasets of brGDGTs in lake sediments and soils were additionally compiled for comparison. Distinct brGDGT distributions in Chilean lakes and soils indicate minimal bias from soil inputs to the lacustrine sediments as well as *in situ* lacustrine production of brGDGTs, which supports the use of brGDGTs in lake sediments as reliable paleotemperature proxies in the region. The ΣIIIa/ΣIIa ratio, initially promising as a brGDGT source indicator in marine settings, shows global complexities in lacustrine settings, challenging the establishment of universal thresholds for source apportionment. That said, we show that the ratio can be successfully applied in Chilean lake surface sediments. Direct comparisons with watershed soils and further research are crucial for discerning brGDGT sources in lake sediments and improving paleotemperature reconstructions on regional and global scales moving forward. Overall, this study contributes valuable insights into brGDGT variability, essential for accurate paleoreconstructions.

KEYWORDS

biomarker, branched GDGTs, lake, soil, Chile

1 Introduction

Quantitative reconstructions of past continental climates are crucial for understanding climate change and informing climate models. Branched glycerol dialkyl glycerol tetraethers (brGDGTs), cell membrane-spanning lipids unique to bacteria, have been suggested as a universal continental paleothermometer as they exhibit strong correlations with environmental variables, especially temperature (e.g., Sinninghe Damsté et al., 2000; Weijers et al., 2006; Chen et al., 2018; 2022; Halamka et al., 2023). The responsiveness of these lipids to changing conditions suggests they can serve as sensitive indicators of past climate variations, allowing for quantitative reconstructions of temperature changes. In particular, brGDGTs preserved in lake sediments offer high-resolution records of past temperature changes (Castañeda and Schouten, 2011; Schouten et al., 2013). Initially, it was thought that these compounds were derived from watershed soils and transported to lakes via erosion and runoff but *in situ* production in lakes is now evident (Tierney and Russell, 2009; Tierney et al., 2012; Wang et al., 2012; Buckles et al., 2014a; Buckles et al., 2014b; Loomis et al., 2014; Peterse et al., 2014; Weber et al., 2015; Hu et al., 2016; Qian et al., 2019; Yao et al., 2020; Wu et al., 2021; Zhang et al., 2021; Zhao et al., 2021; Raberg et al., 2022).

Differences in how brGDGTs respond to temperature in lakes, compared to soils and peats, have led to the development of lake-specific temperature calibration models (Tierney et al., 2010; Zink et al., 2010; Pearson et al., 2011; Sun et al., 2011; Loomis et al., 2012; Wang et al., 2016; 2021; Dang et al., 2018; Russell et al., 2018; Martínez-Sosa et al., 2021; Raberg et al., 2021; Lei et al., 2023; O'Beirne et al., 2023; Zhao et al., 2023). These calibrations aim to account for the unique responses of brGDGTs within lacustrine environments. That said, the lack of a robust lacustrine end-member brGDGT signal means that the relative contributions of lake and soil sources to lacustrine sedimentary lipid pools remain uncertain (e.g., Tierney et al., 2012; Buckles et al., 2014a; Wang et al., 2023). Consequently, the potential for calibration biases due to different sources of brGDGTs poses a significant challenge for the application of brGDGT-based paleothermometry. Indeed, it has long been known that soil-based calibrations do not accurately reconstruct temperature from lake sediments (Blaga et al., 2010; Tierney et al., 2010; Sun et al., 2011; Loomis et al., 2012). Thus, there is a need to understand the relative contributions of *in situ* lacustrine production and soil input, as well as how varying source contributions may impact the use of brGDGTs as temperature proxies in lakes.

The ΣIIIa/ΣIIa ratio was initially proposed to distinguish the origins of brGDGTs in marine sediments. In a global analysis, 90% of soils had a ΣIIIa/ΣIIa ratio below 0.59, while 90% of marine sediments had a ratio exceeding 0.92 (Xiao et al., 2016). This contrast highlights the potential for identifying the origins of brGDGTs in aquatic environments. The ΣIIIa/ΣIIa ratio was first applied to Lake St. Front sediments and watershed soils (Martin et al., 2019) where it was found to be a reliable indicator for tracking the varying abundances of soil-sourced brGDGTs using the ratio cutoff values established for marine sediments (Xiao et al., 2016). The ratio has since been applied in Lake Höglwörth, Southern Germany, although without additional comparison of surrounding watershed soils (Acharya et al., 2023). This ratio clearly offers promise but needs to be further tested to assess its reliability before it is widely applied to lake sediments as a brGDGT source indicator.

In this regard, we analyzed the distributions of brGDGTs in 15 lake surface sediments and corresponding watershed soils from central-south Chile—a region with limited availability of historical climate observations where proxies and paleoclimate records thus become crucial in understanding past climate variability. We also compare the validity of the established marine thresholds of the ΣIIIa/ΣIIa ratio when applied to 1) the Chilean samples; 2) samples from four previously published studies from China and the Eastern Canadian Arctic and 3) samples in a global compilation of 692 lake surface sediment samples and 773 soil samples.

2 Materials and methods

2.1 Study location and sample collection

Fifteen paired (30 total) lake surface sediment (0–1 cm) and corresponding watershed soil (0–5 cm) samples were collected in January 2017, 2018, and 2019 from central-south Chile, spanning a latitudinal range from 38° to 44°S (Figure 1). Coordinates for sampling sites are available in Supplementary Table S1.

2.2 Sample preparation and instrumental analysis

Lake surface sediments and soils (with prior sieving, 2 mm mesh, of soils) were freeze-dried, homogenized, and extracted to obtain extractable lipids. To obtain the Total Lipid Extract (TLE) samples were extracted either via Automated Solvent Extractor (Dionex ASE 350) at the University of Pittsburgh or via Microwave Assisted Extractor (Milestone Ethos Easy) at the Universidad Católica de la Santísima Concepción. The TLE were then separated by Solid Phase Extraction using aminopropyl columns as described in Russell and Werne (2007), and the neutral fraction further separated by alumina column chromatography, following the procedures outlined in Powers et al. (2004). Polar fractions were filtered via 0.45 mm PTFE filters prior to instrumental analysis.

The analysis of brGDGTs involved high-performance liquid chromatography-atmospheric pressure chemical ionization-mass spectrometry (HPLC-APCI-MS), as detailed in Hopmans et al. (2016). In brief, a Thermo Ultimate 3000 series LC with a silica pre-column and two HILIC silica columns (BEH HILIC, 2.1 × 150 mm x 1.7 μm; Waters) in series, maintained at 30°C, was coupled to a Thermo TSQ triple quadrupole MS with an APCI source. The positive ion APCI settings included sheath gas (N2) at 20 AU, auxiliary gas (N2) at 2 AU, ion transfer tube temperature at 275°C, and vaporizer temperature at 375°C. Mass scanning ranged from 700 to 1300 m/z at a scan rate of 500 Da/s, with a Q1 resolution of 0.7 full width at half maximum.

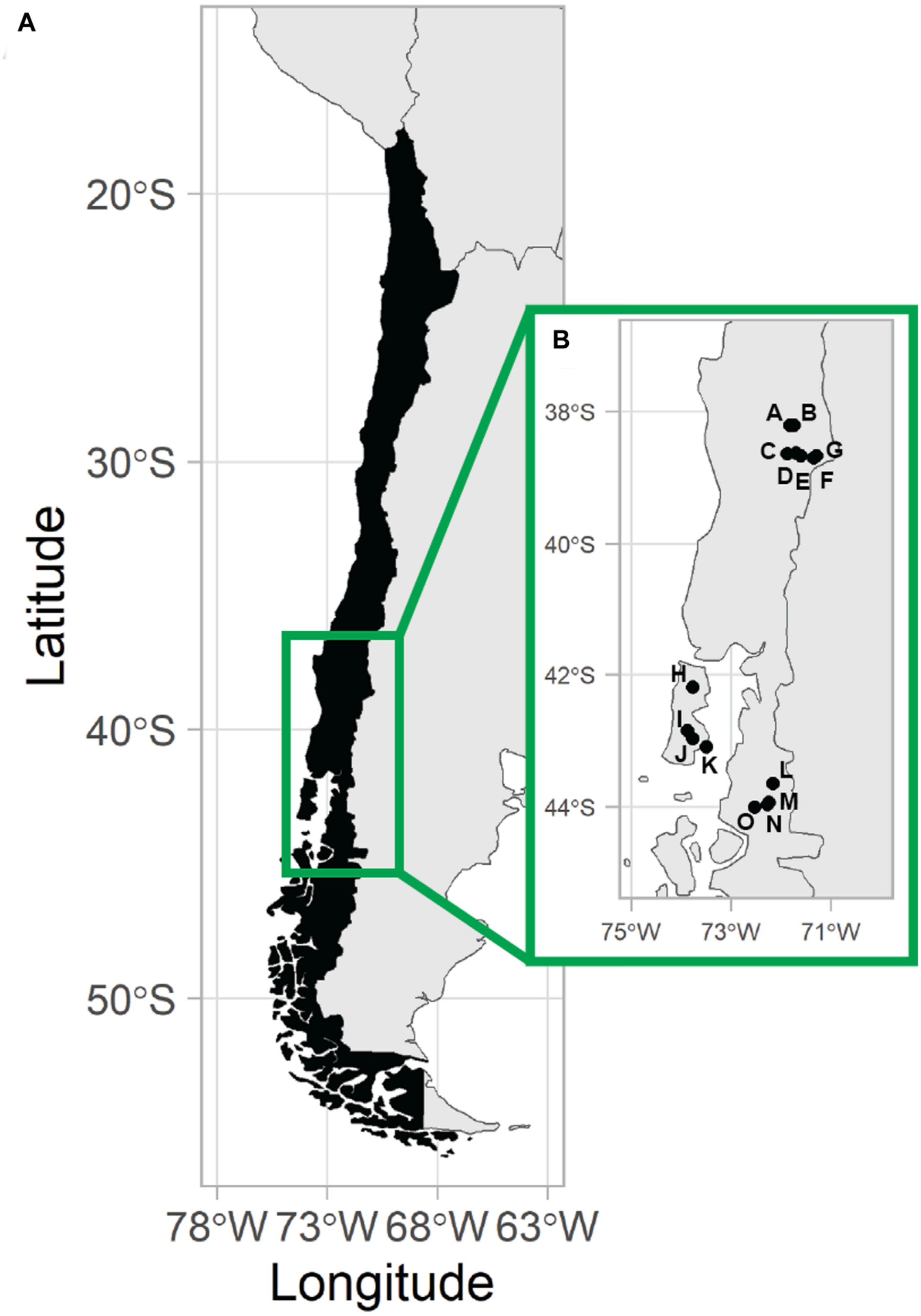

FIGURE 1
Map of sample locations in Chile. **(A)** West coast of South America with the country of Chile highlighted in black. **(B)** Zoom in on sample locations. The letters A–O correspond to panels in Figure 2.

BrGDGTs were identified by comparing their relative retention times and mass spectra with published reference values (e.g., De Jonge et al., 2013; Hopmans et al., 2016). The areas corresponding to individual brGDGTs were integrated from the total ion chromatogram (TIC) using Xcalibur software with Genesis integration. Peak areas were integrated with a minimum signal-to-noise ratio (S/N) cutoff of 3:1 to ensure data integrity.

Analysis of n-alkanes was described in Contreras et al. (2023).

2.3 Ratio calculations

The fractional abundance (fA) of each of the brGDGTs was calculated according to Eq. 1 and are available in Supplementary Table S1.

$$fA_x = \frac{(x)}{(\Sigma brGDGTs)} \tag{1}$$

where x = the integrated peak area of an individual brGDGT.

The ΣIIIa/ΣIIa (Xiao et al., 2016) was calculated using the fAs of brGDGT IIIa and IIa isomers (Eq. 2).

$$\frac{\Sigma \text{IIIa}}{\Sigma \text{IIa}} = \frac{(\text{IIIa} + \text{IIIa}')}{(\text{IIa} + \text{IIa}')} \tag{2}$$

The Methylation of 5-Methyl Branched Tetraethers (MBT'_{5ME}) ratio was calculated (Eq. 3) using the fAs of the corresponding brGDGTs (De Jonge et al., 2014).

$$\text{MBT}'_{5\text{ME}} = \frac{(\text{Ia} + \text{Ib} + \text{Ic})}{(\text{Ia} + \text{Ib} + \text{Ic} + \text{IIa} + \text{IIb} + \text{IIc} + \text{IIIa})} \tag{3}$$

2.4 Published datasets of brGDGTs in lake surface sediments and soils

Data from four studies (Yao et al., 2020; Wu et al., 2021; Raberg et al., 2022; Wang et al., 2023) was compiled, focusing on paired lake surface sediment and corresponding watershed soil samples. In all four studies, it was observed that brGDGTs in lake surface sediments predominantly originated from lacustrine sources. Yao et al. (2020) studied lake surface sediments and soils in northeastern China. Wu et al. (2021) focused on Lake Yangzonghai and its surrounding watershed soils in southwestern China and found that the distribution of lacustrine brGDGTs correlated significantly with bottom water dissolved oxygen (DO) concentration, which is in turn linked to water depth. Raberg et al. (2022) examined lakes in the Eastern Canadian Arctic. Wang et al. (2023) investigated paired lake surface sediments and soils across China.

Global lake surface sediment brGDGT data was compiled from several previously published studies and includes 65 samples from Russell et al. (2018), 35 samples from Dang et al. (2018), 36 samples from Weber et al. (2018), one sample from Miller et al. (2018), one sample from Qian et al. (2019), one sample from Ning et al. (2019), one sample from Cao et al. (2020), two samples from Dugerdil et al. (2021), 43 samples from Raberg et al. (2021), 157 samples from Martínez-Sosa et al. (2021), 107 samples from Kou et al. (2022), 102 samples from Lei et al. (2023), 91 samples from Zhao et al. (2023), and 50 samples from O'Beirne et al. (2023).

Global soil brGDGT data was downloaded as Supplementary Material from Véquaud et al. (2022). The dataset includes 128 samples from De Jonge et al. (2014), 76 samples from Dearing et al. (2020), 27 samples from Xiao et al. (2015), 26 samples from Yang et al. (2015), 44 samples from Lei et al. (2016), 148 samples from Wang et al. (2016), 27 samples from Ding et al. (2015), 11 samples from Huguet et al. (2019), 52 samples from Véquaud et al. (2021a), and 49 samples from Véquaud et al. (2021b).

2.5 Data analysis

Data analysis was completed using the free and open-source software **R** (v. 4.3.1; R Core Team, 2023) and **RStudio** (v. 2023.9.1.494; Posit team, 2023). Principal Component Analysis (PCA) was applied to the fAs of brGDGTs to uncover any underlying structure or patterns in how brGDGTs were distributed between lake surface sediments and watershed soils. PCA was completed using the **stats** package (v. 4.3.1; R Core Team, 2023) and plotted using **ggplot2** (v. 3.4.3; Wickham, 2016). Data was scaled and centered before running the PCA. Additional statistical analyses were completed using the **ggstatsplot** package (v. 0.12.0: Patil, 2021).

3 Results and discussion

3.1 Contrasting brGDGT distributions in lake surface sediments and watershed soils

In both lake surface sediments and watershed soils five of the fifteen commonly reported brGDGTs (IIc', IIIb, IIIb', IIIc, and IIIc') were below detection (Figure 2), which is not uncommon in lake systems (Lei et al., 2023; O'Beirne et al., 2023). The distributions of the ten detected brGDGTs in lake surface sediments and corresponding watershed soils display distinctly different distributions (Figure 2). The most striking difference among the distributions of brGDGTs between lake surface sediments and their watershed soils is the predominance of brGDGTs IIIa and IIIa' in lake surface sediments and brGDGT Ia in soils. This distinction is further emphasized in the PCA on combined lake and soil samples, where soils cluster predominantly in quadrant I, aligned with brGDGT Ia, while lake surface sediments cluster in quadrant III, associated with brGDGTs IIIa and IIIa' (Figure 3A). The contrasting distributions of brGDGTs between lake surface sediments and their corresponding watershed soils shows that there is *in situ* production of brGDGTs in lakes (Figures 2, 3A). Even though lake sediments comprise both soil and lacustrine sourced brGDGTs, the prevalence of brGDGTs IIIa and IIIa' in lake surface sediments, juxtaposed with the dominance of brGDGT Ia in soils, signifies that lakes and soils in Chile have distinctly different brGDGT distributions. We hypothesize that this observation is likely due to distinct roles and processes governing brGDGT production and preservation in these two environments, especially because this pattern is consistent with observations from diverse locations (e.g., Tierney et al., 2010; Buckles et al., 2014a; Buckles et al., 2014b; Loomis et al., 2014; Weber et al., 2015; Hu et al., 2016; Li et al., 2017; Yao et al., 2020; Wang et al., 2021).

The clear differences in brGDGT distributions between Chilean lake surface sediments and soils indicate that we can potentially distinguish between these two sources in lake sediment records. This capability would enable us to track the changing contributions of each source over time and, if needed, adjust for minor inputs from one source if we can establish appropriate proxies.

3.2 Comparison of the ΣIIIa/ΣIIa ratio in lakes and soils

The ΣIIIa/ΣIIa ratio in Chilean soils follows the thresholds established in marine sediments for soil- and marine-sourced brGDGTs (Figure 4A). Notably, all the soil samples fall below the ΣIIIa/ΣIIa threshold of 0.59, a criterion typically used to identify soil-derived brGDGTs (Xiao et al., 2016). Further, all but two lake surface sediment samples have ΣIIIa/ΣIIa values above the 0.59 threshold of soils. Even so, the ΣIIIa/ΣIIa values of the lake surface sediments and soils of these two samples (Cipreces and

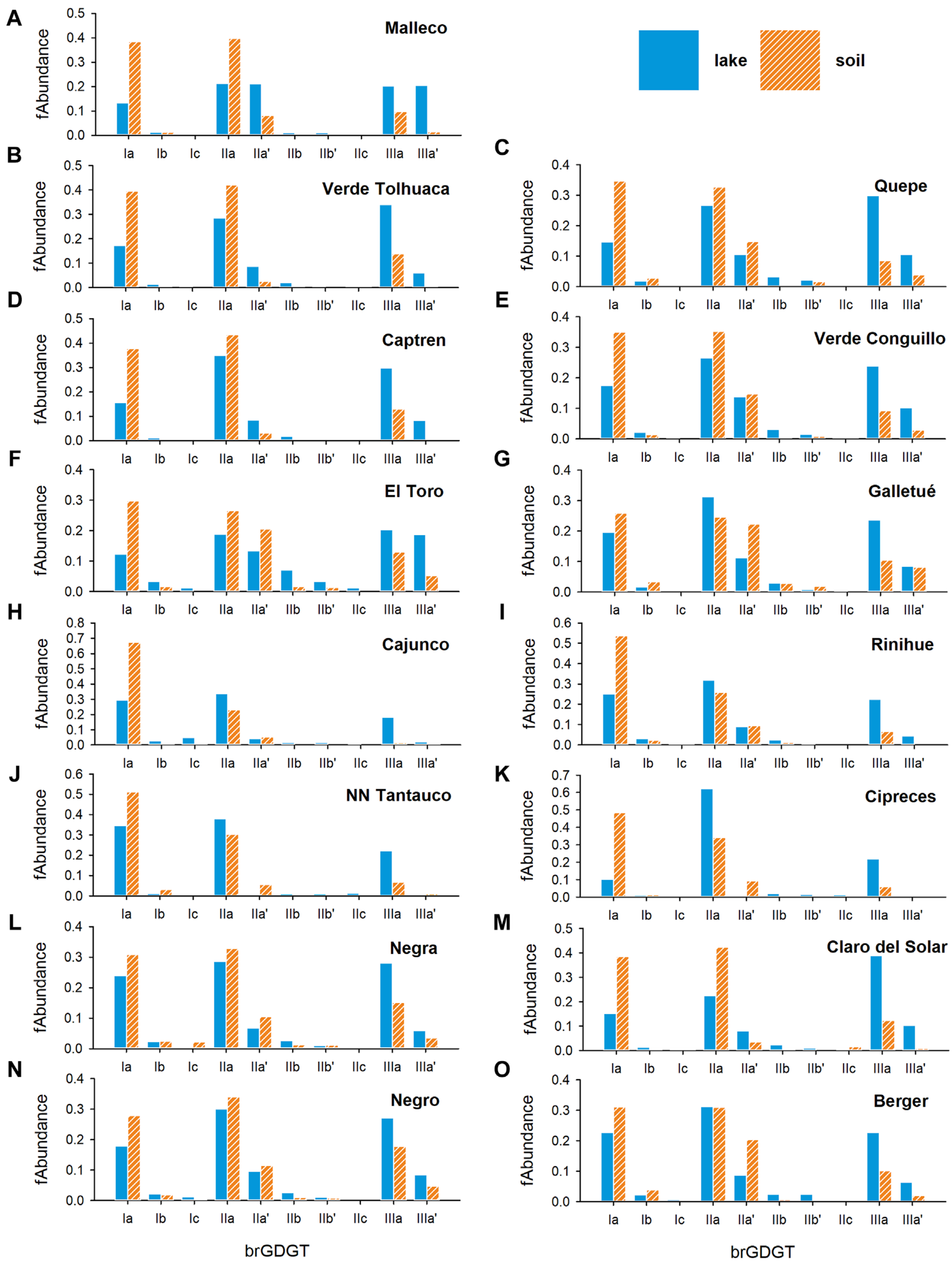

FIGURE 2
Fractional abundances of brGDGTs from lake surface sediments and their respective watershed soils. **(A–O)** Sampling sites from north to south in Chile.

Cajunco) are distinctly different (Table 1). Further, a within subjects robust *t*-test reveals that the ΣIIIa/ΣIIa ratios between each of the paired lake surface sediment and soil samples are significantly different (t_{Yuen} (8) = 9.13, p = 1.66e-05, $\hat{\delta}^{AKP}_{R\text{-}avg}$ = 2.40, $CI_{95\%}$ [1.89, 5.43], n_{pairs} = 15). Given that soils adhere to the established ΣIIIa/ΣIIa soil threshold, using it as a criterion to evaluate the influence of soil-sourced brGDGTs on lacustrine paleorecords in Chilean lakes and, consequently, the effects on paleotemperature

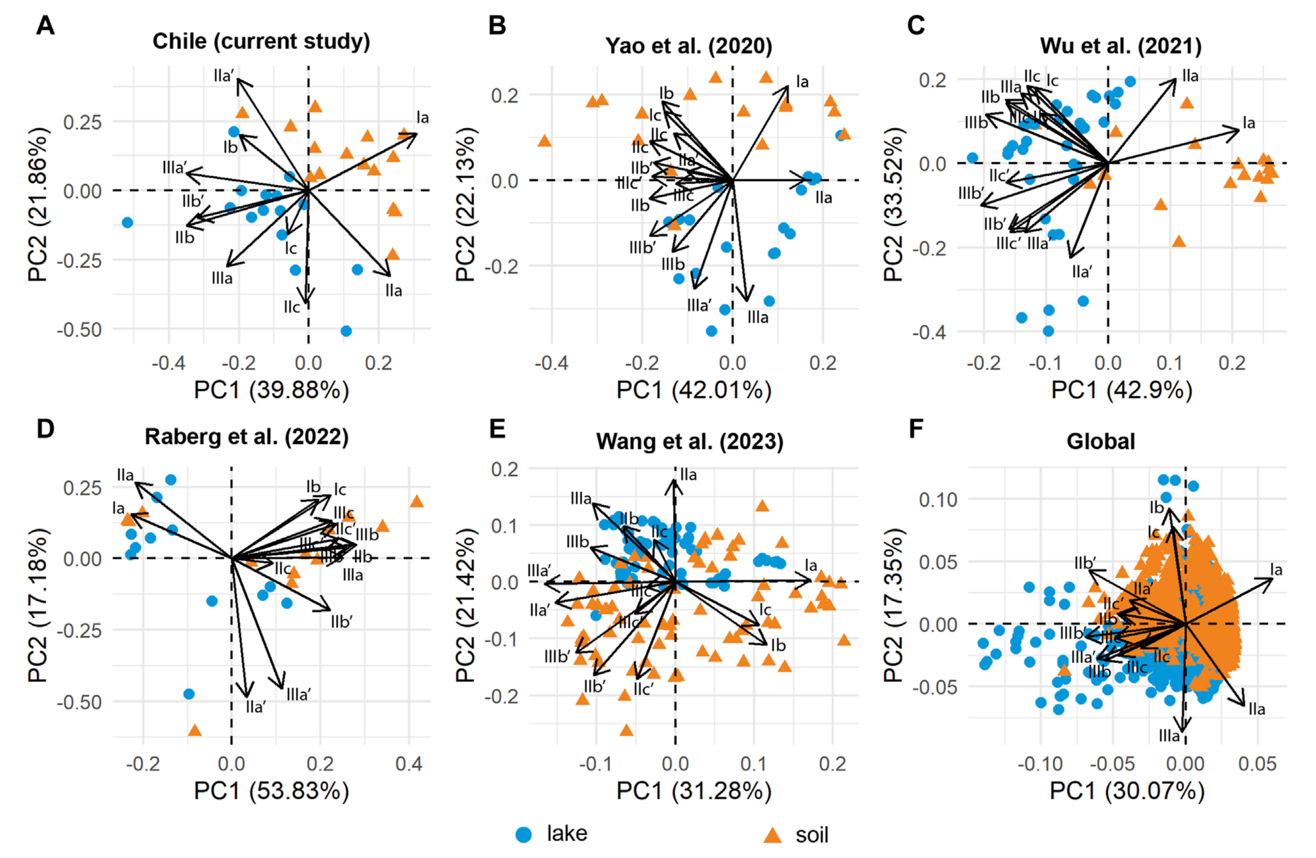

FIGURE 3
Principal component analysis (PCA) bi-plots of principal component 1 (PC1) and principal component 2 (PC2) showing the scores of each sample (lakes - blue circles and soils - orange triangles) and the loadings of each brGDGT for each sample set. Vertical and horizontal dashed reference lines indicate where the x- and *y*-intercept are 0. **(A)** Chilean samples. **(B)** Samples from northeastern China (Yao et al., 2020). **(C)** Samples from Lake Yangzonghai in southwestern China (Wu et al., 2021). **(D)** Samples from the Eastern Canadian Arctic (Raberg et al., 2022). **(E)** Samples from across China (Wang et al., 2023). **(F)** Global compilation of lake surface sediment and soil samples.

reconstruction may be beneficial for the majority of Chilean lakes.

When we extend our analysis to previously published paired local and regional datasets as well as the global datasets of lake surface sediments and soils, the distinction between the two sources, as indicated by the established marine thresholds of ΣIIIa/ΣIIa ratio, becomes less clear (Figures 4B–F). Although four prior studies (Yao et al., 2020; Wu et al., 2021; Raberg et al., 2022; Wang et al., 2023) investigated paired lake surface sediments and soils and concluded that brGDGTs in lake sediments primarily originated from lacustrine sources, the effectiveness of using the ΣIIIa/ΣIIa ratio to differentiate between sources varies. Specifically, while the samples from Yao et al. (2020) adhere to the established threshold for soil-derived brGDGTs, the other three studies do not (Figures 4B–E). Furthermore, there is significant overlap between lake surface sediments and soils in the PCA bi-plots for the studies where the ΣIIIa/ΣIIa ratio fails, i.e., Wu et al. (2021), Raberg et al. (2022) and Wang et al. (2023) (Figures 3B–E). These observations provide strong evidence that the established marine thresholds for aquatic and soil origins are not universally applicable to lake sediments and relying on this ratio alone may not be enough to correctly characterize source contributions.

The compilation of globally distributed 692 lake surface sediments and 773 soils shows that approximately 85% of soil samples and 49% of lake samples display ΣIIIa/ΣIIa ratios below the 0.59 threshold of soils (Figure 4F). In contrast, only 35% of lake samples have ΣIIIa/ΣIIa values exceeding the upper threshold used to identify marine-derived brGDGTs (i.e., ΣIIIa/ΣIIa >0.92; Xiao et al., 2016). Not only does this contrast with the findings for marine sediments where 90% of marine sediments had ΣIIIa/ΣIIa values >0.92, but also shows considerable overlap between soil and lake surface sediment samples. This overlap complicates the use of the ΣIIIa/ΣIIa ratio in lake sediments overall. This presents two potential scenarios: either 1) almost half of global lakes are significantly influenced by soil-derived brGDGTs, or 2) the ΣIIIa/ΣIIa ratio does not offer as distinct a differentiation for lakes as it does for marine sediments.

The first scenario contradicts a prior study which suggested that only ca. 10% of global lakes are significantly affected by soil-sourced brGDGTs, as extrapolated from a calculation based on 26 Chinese lakes that assumes that crenarchaeol, its isomer crenarchaeol', and C_{33} *n*-alkane can be used as tracers for soil input of brGDGTs (Wang et al., 2023). This calculation may be an oversimplification in certain contexts. Specifically, in our Chilean samples, we did

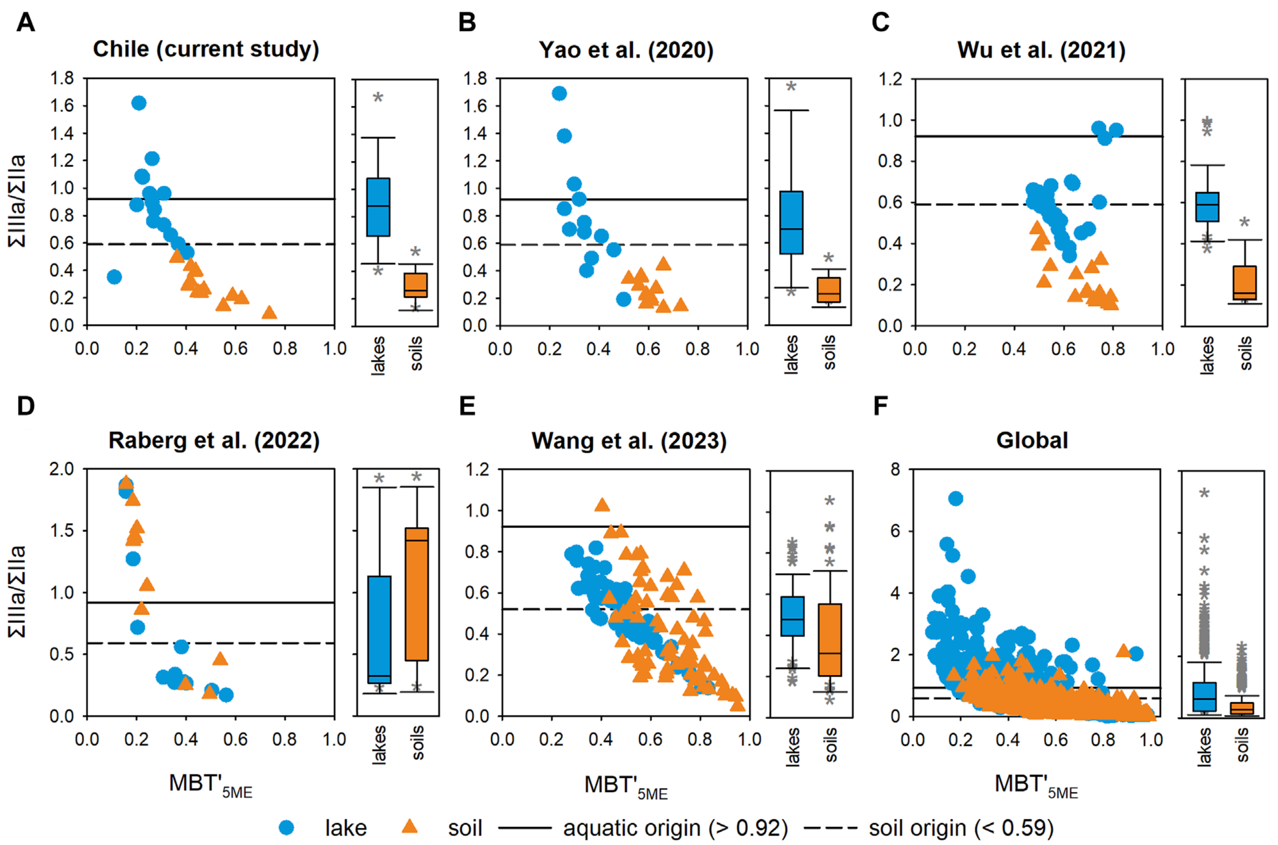

FIGURE 4
The ΣIIIa/ΣIIa ratio applied to each sample set. The horizontal dashed line denotes the upper limit of soil-sourced brGDGTs and the solid line denotes the lower limit of marine/aquatic-sourced brGDGTs as established for marine sediments by Xiao et al. (2016). **(A)** Chilean samples. **(B)** Samples from northeastern China (Yao et al., 2020). **(C)** Samples from Lake Yangzonghai in southwestern China (Wu et al., 2021). **(D)** Samples from the Eastern Canadian Arctic (Raberg et al., 2022). **(E)** Samples from across China (Wang et al., 2023). **(F)** Global compilation of lake surface sediment and soil samples.

not observe a significant difference in C_{33} n-alkane concentrations between lakes and soils (within subjects robust t-test; t_{Yuen} (8) = −1.62, p = 0.14, $\hat{\delta}^{AKP}_{R\text{-}avg}$ = −0.51, $CI_{95\%}$ [−1.20, −5.68e-03], n_{pairs} = 15). This suggests that lake sediments may be dominated by lipids originating from soil sources. However, the distribution of brGDGTs between the two archives shows significant differences, contradicting the data on C_{33} n-alkanes. Consequently, accounting for the C_{33} n-alkane in the equation may lead to an overestimation of soil-sourced brGDGTs and skew paleotemperature reconstructions that attempt to account for their influence if applied to Chilean lakes.

A probable explanation for this discrepancy and something to consider in future attempts at calculating source contributions are the delivery mechanisms of the two lipid classes. Specifically, leaf waxes are delivered to lake sediments via three primary mechanisms: attached to deposited leaves, wind-driven abrasion and deposition, and the erosion and deposition of soil-derived waxes (Diefendorf and Freimuth, 2017). In contrast, soil-sourced brGDGTs are mainly transported to lakes through erosion and runoff (Blaga et al., 2010 and references therein) and to a lesser extent wind (Fietz et al., 2013; Yamamoto et al., 2016). Changes in the primary delivery mechanisms of each lipid class would clearly affect the proportions of each that are measured in lake sediments, as the mechanisms of each may not be directly comparable to one another in both contemporary and historical contexts.

Taken altogether, the second scenario offers the most parsimonious explanation—the ΣIIIa/ΣIIa ratio does not provide as clear a distinction for lake sediments as it does for marine sediments. This inference is supported not only by the substantial overlap observed in the global datasets of lake surface sediments and soils but is also underscored by the local and regional paired studies. These studies demonstrated that brGDGTs in lake sediments originated primarily from lacustrine sources, despite there being significant overlap between soils and lake surface sediments when the ΣIIIa/ΣIIa ratio is applied (Figures 4B–D).

3.3 Influences on the ΣIIIa/ΣIIa ratio in lake sediments

Complications in utilizing the ΣIIIa/ΣIIa ratio to distinguish between lake surface sediments and soils also arise due to the influence of water depth on the abundance of brGDGT IIIa relative to IIa. Previous research (Yao et al., 2020; Stefanescu et al., 2021) indicates that the abundance of brGDGT IIIa increases

TABLE 1 ΣIIIa/ΣIIa ratio for Chilean lake surface sediments and watershed soils.

Map ID	Identifier	Lake	Soil
A	Malleco	0.96	0.24
B	Verde Tolhuaca	1.08	0.32
C	Quepe	1.08	0.26
D	Captren	0.88	0.29
E	Verde Conguillo	0.84	0.24
F	El Toro	1.21	0.39
G	Galletué	0.76	0.40
H	Cajunco	0.53	0.08
I	Rinihue	0.66	0.19
J	NN Tantauco	0.59	0.22
K	Cipreces	0.35	0.14
L	Negra	0.96	0.43
M	Claro del Solar	1.62	0.29
N	Negro	0.90	0.49
O	Berger	0.73	0.24

with greater water depth in lakes. However, in the Chilean lakes studied, ranging from 6.5 to 41.2 m in depth (mean = 21.02 m; Supplementary Table S1), we found no correlation between water depth and the fA of brGDGT IIIa ($t_{Student}$ (13) = 1.52, p = 0.15, $\hat{r}$ $_{Winzorized}$ = 0.39, $CI_{95\%}$ [−0.15, 0.75], n_{pairs} = 15), nor between water depth and the ΣIIIa/ΣIIa ratio ($t_{Student}$ (13) = 0.97, p = 0.35, $\hat{r}$ $_{Winzorized}$ = 0.26, $CI_{95\%}$ [−0.29, 0.68], n_{pairs} = 15).

Further, when analyzing data from published studies, we found no consistent trend. For instance, Yao et al. (2020) observed a significant positive correlation between water depth and the fA of brGDGT IIIa ($t_{Student}$ (11) = 3.75, p = 3.23e-03, $\hat{r}$ $_{Winzorized}$ = 0.75, $CI_{95\%}$ [0.34, 0.92], n_{pairs} = 13), as well as the ΣIIIa/ΣIIa ratio ($t_{Student}$ (11) = 5.27, p = 2.63e-04, $\hat{r}$ $_{Winzorized}$ = 0.85, $CI_{95\%}$ [0.55, 0.95], n_{pairs} = 13), in lakes from eastern China. However, in Lake Yangzonghai (Wu et al., 2021) southwestern China, while there was a significant positive correlation between water depth and the fA of brGDGT IIIa ($t_{Student}$ (33) = 4.90, p = 2.50e-05, $\hat{r}$ $_{Winzorized}$ = 0.65, $CI_{95\%}$ [0.40, 0.81], n_{pairs} = 35), there was a significant negative correlation between water depth and the ΣIIIa/ΣIIa ratio ($t_{Student}$ (33) = −3.16, p = 3.36e-03, $\hat{r}$ $_{Winzorized}$ = −0.48, $CI_{95\%}$ [-0.70, −0.18], n_{pairs} = 35), contrary to findings from lakes in eastern China. In a broader study across China (Wang et al., 2023), only weak correlations were found between water depth and the fA of brGDGT IIIa ($t_{Student}$ (73) = 2.43, p = 0.02, $\hat{r}$ $_{Winzorized}$ = 0.27, $CI_{95\%}$ [0.05, 0.47], n_{pairs} = 75], npairs = 75) and the ΣIIIa/ΣIIa ratio ($t_{Student}$ (73) = 0.75, p = 0.46, $\hat{r}$ $_{Winzorized}$ = 0.09, $CI_{95\%}$ [-0.14, 0.31], n_{pairs} = 75). These findings suggest that the relationship between brGDGT IIIa abundance and water depth may be site-specific and not universal.

Additionally, two of the studies provided dissolved oxygen (DO) concentrations (Wu et al., 2021; Wang et al., 2023). Correlation analysis showed a weak positive correlation between DO and the ΣIIIa/ΣIIa ratio in Lake Yangzonghai ($t_{Student}$ (33) = 2.28, p = 0.03, $\hat{r}$ $_{Winzorized}$ = 0.37, $CI_{95\%}$ [0.04, 0.62], n_{pairs} = 35), but no significant correlation was found in lakes from across China ($t_{Student}$ (73) = 0.89, p = 0.38, $\hat{r}$ $_{Winzorized}$ = 0.10, $CI_{95\%}$ [−0.13, 0.32], n_{pairs} = 75). Thus, it appears that DO concentrations do not significantly influence the ΣIIIa/ΣIIa ratio.

3.4 The ΣIIIa/ΣIa ratio as a source indicator

We also explored the potential use of the ΣIIIa/ΣIa ratio (the sum of the fractional abundances of brGDGTs IIIa and IIIa' divided by the fractional abundance of brGDGT Ia) as a source indicator. This exploration was prompted by the dominance and alignment of brGDGTs IIIa and IIIa' in Chilean lake surface sediments and in other paired studies, contrasting with the prevalent alignment of watershed soils with brGDGT Ia in the PCA bi-plot (Figure 3A). The ΣIIIa/ΣIa ratio yields similar outcomes to the ΣIIIa/ΣIIa ratio in Chilean lake surface sediments and soils, maintaining a distinct separation between them (Figure 5A). However, when applied to the other paired studies as well as the global lake surface sediments and soils, this ratio fails to provide a clearer distinction than the ΣIIIa/ΣIIa ratio (Figures 5B–F). This lack of clarity, for both ratios, can be attributed to the greater overlap in brGDGT distributions between the two archives, as evidenced in the respective lake surface sediment and soils PCA bi-plot (Figures 3B–F).

3.5 Implications

The findings of this study provide valuable insights into the distribution of brGDGTs in Chilean lake surface sediments and their corresponding watershed soils. Understanding these distributions is essential for interpreting paleoclimatological conditions accurately.

To assess the impact of soil-sourced brGDGTs on lacustrine temperature reconstruction in Chile, we employed both lake surface sediment brGDGTs and soil brGDGTs in five recent lacustrine-based temperature calibration models (Martínez-Sosa et al., 2021; Raberg et al., 2021; O'Beirne et al., 2023; Zhao et al., 2023). The results revealed a significant discrepancy: using soil brGDGTs in the models led to a substantial overestimation (by > 10°C) of mean annual air temperature (MAAT) compared to using lake surface sediment brGDGTs (Figure 6). This finding underscores the necessity of employing environment-specific calibration models, as advocated in previous studies (Tierney et al., 2010; Zink et al., 2010; Pearson et al., 2011; Sun et al., 2011; Loomis et al., 2012; Wang et al., 2016; 2021; Dang et al., 2018; Russell et al., 2018; Martínez-Sosa et al., 2021; Raberg et al., 2021; Lei et al., 2023; O'Beirne et al., 2023; Zhao et al., 2023). Additionally, these results highlight the necessity of assessing the origin of brGDGTs in

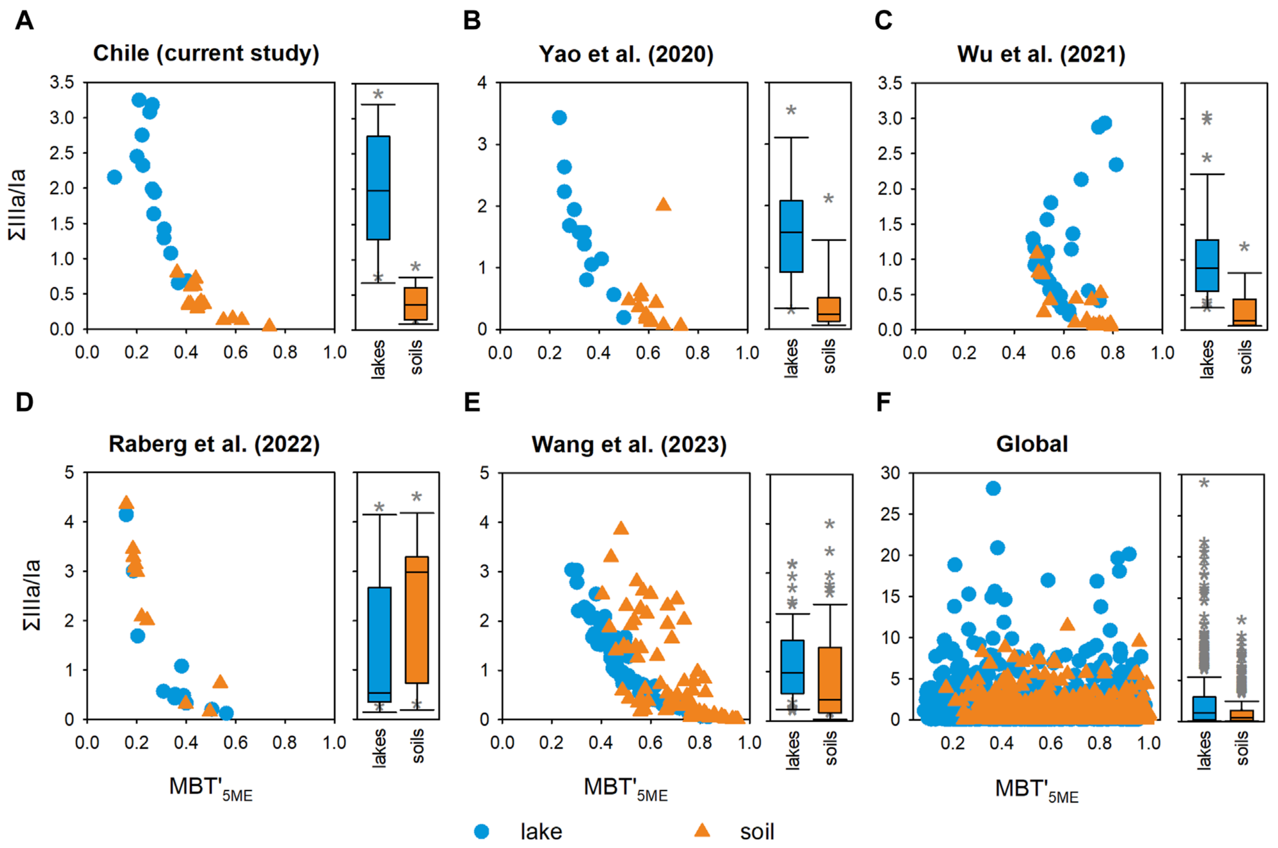

FIGURE 5
The ΣIIIa/ΣIa ratio applied to each sample set. **(A)** Chilean samples. **(B)** Samples from northeastern China (Yao et al., 2020). **(C)** Samples from Lake Yangzonghai in southwestern China (Wu et al., 2021). **(D)** Samples from the Eastern Canadian Arctic (Raberg et al., 2022). **(E)** Samples from across China (Wang et al., 2023). **(F)** Global compilation of lake surface sediment and soil samples.

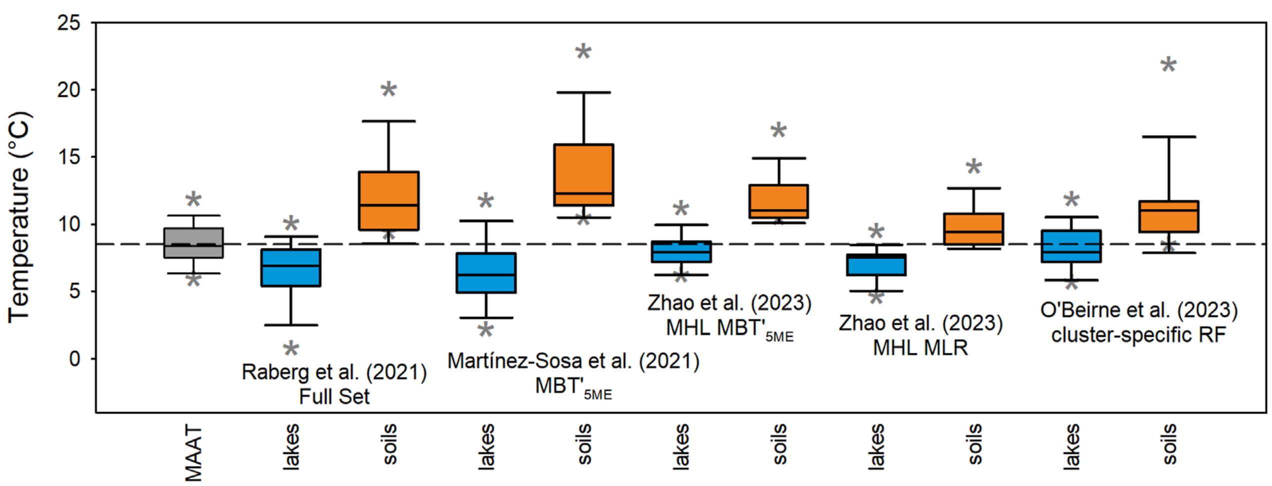

FIGURE 6
Boxplot distributions of air temperature (in Celsius) sourced from the CR2MET database (https://www.cr2.cl/datos-productos-grillados) for mean annual air temperature (MAAT) along with temperature reconstructions derived from five recent lacustrine-based temperature calibration models (Raberg et al., 2021 [Full set]; Martínez-Sosa et al., 2021 [MBT'$_{5ME}$]; Zhao et al., 2023 [mid-high latitude (MHL) MBT'$_{5ME}$ and MHL multiple linear regression (MLR); O'Beirne et al., 2023 [cluster-specific random forest (RF)]). In the plot, 'lakes' depict the temperature range when brGDGTs from lake sediments were utilized in the calibration models, while 'soils' represent the reconstructed temperature range when corresponding watershed soils were employed in the calibration models. For the sample locations in Chile, there are no months where air temperature is below freezing, therefore MAAT is equal to months above freezing (MAF) temperature.

lake sediments and applying the most appropriate environment-specific calibration model, as overestimating soil-sourced brGDGTs in lake sediments could skew temperature reconstructions towards much warmer temperatures which would lead to incorrect interpretations—this may be especially important during periods of significant environmental change, such as glacial-interglacial transitions, or other periods of vegetation change or human impacts as noted by Martin et al. (2019). Therefore, it is crucial to carefully account for source changes in paleorecords and consider contemporary distribution differences between sources, along with other proxy data like carbon-to-nitrogen ratios, trace metals, and sediment grain size to substantiate source change interpretations.

In our Chilean samples, the adherence of soils to established threshold for the ΣIIIa/ΣIIa ratio supports its use in evaluating the impact of soil-sourced brGDGTs on lacustrine sediment core records and brGDGT-based paleotemperature reconstructions. However, applying these marine thresholds globally presents challenges, as there is significant overlap between soil and lake samples, suggesting a potentially significant influence of soil-derived brGDGTs in almost half of the world's lakes. The limitations of established marine thresholds are further highlighted by several studies showing considerable overlap between paired lake sediments and soils, despite brGDGTs in lake sediments originating primarily from lacustrine sources (Yao et al., 2020; Wu et al., 2021; Raberg et al., 2022; Wang et al., 2023). Hence, caution is warranted when relying solely on established marine thresholds for discerning brGDGT sources using the ΣIIIa/ΣIIa ratio. Instead, establishing local or regional thresholds through direct comparisons between brGDGT distributions in lakes and corresponding watershed soils is more advisable.

Data availability statement

The original contributions presented in the study are included in the article/Supplementary Material, further inquiries can be directed to the corresponding authors.

Author contributions

MB: Conceptualization, Data curation, Formal Analysis, Investigation, Validation, Visualization, Writing–original draft, Writing–review and editing. WS: Data curation, Formal Analysis, Investigation, Validation, Writing–review and editing. SC: Funding acquisition, Investigation, Project administration, Resources, Supervision, Writing–review and editing. AA: Investigation, Writing–review and editing. ET: Investigation, Writing–review and editing. JM: Investigation, Writing–review and editing. JW: Conceptualization, Funding acquisition, Investigation, Project administration, Resources, Supervision, Writing–review and editing.

Funding

The author(s) declare that financial support was received for the research, authorship, and/or publication of this article. Funding for this project was provided by the Agencia Nacional de Investigación y Desarrollo de Chile (ANID) Fondecyt 1160719, 1190398, and 1201277 to SC and AA The University of Pittsburgh provided additional support through a Central Research Development Fund grant to JW. An Andrew Mellon Predoctoral Fellowship through the University of Pittsburgh provided research support to WS.

Acknowledgments

We thank the Corporación Nacional Forestal (CONAF) for providing access to National Parks. We would also like to thank the editor and reviewers for their constructive comments. SC acknowledges the "Fondo Interno para la Adquisición de Equipamiento Científico de la Universidad Católica de la Santísima Concepción—FIAEC 2019," and the FAA (2/2019) received from UCSC to complete this work.

Conflict of interest

The authors declare that the research was conducted in the absence of any commercial or financial relationships that could be construed as a potential conflict of interest.

Publisher's note

Supplementary material

The Supplementary Material for this article can be found online at: https://www.frontiersin.org/articles/10.3389/feart.2024.1383146/full#supplementary-material

References

Acharya, S., Zech, R., Strobel, P., Bliedtner, M., Prochnow, M., and De Jonge, C. (2023). Environmental controls on the distribution of GDGT molecules in Lake Höglwörth, Southern Germany. *Org. Geochem.* 186, 104689. doi:10.1016/j.orggeochem.2023.104689

Blaga, C. I., Reichart, G. J., Schouten, S., Lotter, A. F., Werne, J. P., Kosten, S., et al. (2010). Branched glycerol dialkyl glycerol tetraethers in lake sediments: can they be used as temperature and pH proxies? *Org. Geochem.* 41, 1225–1234. doi:10.1016/j.orggeochem.2010.07.002

Brand, A., Allen, L., Altman, M., Hlava, M., and Scott, J. (2015). Beyond authorship: attribution, contribution, collaboration, and credit. *Learn. Pub.* 28, 151–155. doi:10.1087/20150211

Buckles, L. K., Weijers, J. W. H., Tran, X.-M., Waldron, S., and Sinninghe Damsté, J. S. (2014). Provenance of tetraether membrane lipids in a large temperate lake (Loch Lomond, UK): implications for glycerol dialkyl glycerol tetraether (GDGT)-based palaeothermometry. *Biogeosciences* 11, 5539–5563. doi:10.5194/bg-11-5539-2014

Buckles, L. K., Weijers, J. W. H., Verschuren, D., and Sinninghe Damsté, J. S. (2014). Sources of core and intact branched tetraether membrane lipids in the lacustrine environment: anatomy of Lake Challa and its catchment, equatorial East Africa. *Geochimica Cosmochimica Acta* 140, 106–126. doi:10.1016/j.gca.2014.04.042

Cao, J., Rao, Z., Shi, F., and Jia, G. (2020). Ice formation on lake surfaces in winter causes warm-season bias of lacustrine brGDGT temperature estimates. *Biogeosciences* 17, 2521–2536. doi:10.5194/bg-17-2521-2020

Castañeda, I. S., and Schouten, S. (2011). A review of molecular organic proxies for examining modern and ancient lacustrine environments. *Quat. Sci. Rev.* 30, 2851–2891. doi:10.1016/j.quascirev.2011.07.009

Chen, Y., Zheng, F., Chen, S., Liu, H., Phelps, T. J., and Zhang, C. (2018). Branched GDGT production at elevated temperatures in anaerobic soil microcosm incubations. *Org. Geochem.* 117, 12–21. doi:10.1016/j.orggeochem.2017.11.015

Chen, Y., Zheng, F., Yang, H., Yang, W., Wu, R., Liu, X., et al. (2022). The production of diverse brGDGTs by an Acidobacterium providing a physiological basis for paleoclimate proxies. *Geochimica Cosmochimica Acta* 337, 155–165. doi:10.1016/j.gca.2022.08.033

Contreras, S., Werne, J. P., Araneda, A., Tejos, E., and Moscoso, J. (2023). Abundance and distribution of plant derived leaf waxes (long chain *n*-alkanes & fatty acids) from lake surface sediments along the west coat of southern South America: implications for environmental and climate reconstructions. *Sci. Total Environ.* 895, 165065. doi:10.1016/j.scitotenv.2023.165065

Dang, X., Ding, W., Yang, H., Pancost, R. D., Naafs, B. D. A., Xue, J., et al. (2018). Different temperature dependence of the bacterial brGDGT isomers in 35 Chinese lake sediments compared to that in soils. *Org. Geochem.* 119, 72–79. doi:10.1016/j.orggeochem.2018.02.008

Dearing, C.-F. E., Tierney, J. E., Peterse, F., Kirkels, F. M. S. A., and Sinninghe Damsté, J. S. (2020). BayMBT: a Bayesian calibration model for branched glycerol dialkyl glycerol tetraethers in soils and peats. *Geochimica Cosmochimica Acta* 268, 142–159. doi:10.1016/j.gca.2019.09.043

De Jonge, C., Hopmans, E. C., Stadnitskaia, A., Rijpstra, W. I. C., Hofland, R., Tegelaar, E., et al. (2013). Identification of novel penta- and hexamethylated branched glycerol dialkyl glycerol tetraethers in peat using HPLC–MS2, GC–MS and GC–SMB-MS. *Org. Geochem.* 54, 78–82. doi:10.1016/j.orggeochem.2012.10.004

De Jonge, C., Hopmans, E. C., Zell, C. I., Kim, J.-H., Schouten, S., and Sinninghe Damsté, J. S. (2014). Occurrence and abundance of 6-methyl branched glycerol dialkyl glycerol tetraethers in soils: implications for palaeoclimate reconstruction. *Geochimica Cosmochimica Acta* 141, 97–112. doi:10.1016/j.gca.2014.06.013

Diefendorf, A. F., and Freimuth, E. J. (2017). Extracting the most from terrestrial plant-derived n-alkyl lipids and their carbon isotopes from the sedimentary record: a review. *Org. Geochem.* 103, 1–21. doi:10.1016/j.orggeochem.2016.10.016

Ding, S., Xu, Y., Wang, Y., He, Y., Hou, J., Chen, L., et al. (2015). Distribution of branched glycerol dialkyl glycerol tetraethers in surface soils of the Qinghai–Tibetan Plateau: implications of brGDGTs-based proxies in cold and dry regions. *Biogeosciences* 12, 3141–3151. doi:10.5194/bg-12-3141-2015

Dugerdil, L., Joannin, S., Peyron, O., Jouffroy-Bapicot, I., Vannière, B., Boldgiv, B., et al. (2021). Climate reconstructions based on GDGT and pollen surface datasets from Mongolia and Baikal area: calibrations and applicability to extremely cold–dry environments over the Late Holocene. *Clim. Past.* 17, 1199–1226. doi:10.5194/cp-17-1199-2021

Fietz, S., Prahl, F. G., Moraleda, N., and Rosell-Mele´, A. (2013). Eolian transport of glycerol dialkyl glycerol tetraethers (GDGTs) off northwest Africa. *Org. Geochem.* 64, 112–118. doi:10.1016/j.orggeochem.2013.09.009

Halamka, T. A., Raberg, J. H., McFarlin, J. M., Younkin, A. D., Mulligan, C., Liu, X., et al. (2023). Production of diverse brGDGTs by Acidobacterium *Solibacter usitatus* in response to temperature, pH, and O_2 provides a culturing perspective on br GDGT proxies and biosynthesis. *Geobiology* 21, 102–118. doi:10.1111/gbi.12525

Hopmans, E. C., Schouten, S., and Sinninghe Damsté, J. S. (2016). The effect of improved chromatography on GDGT-based palaeoproxies. *Org. Geochem.* 93, 1–6. doi:10.1016/j.orggeochem.2015.12.006

Hu, J., Zhou, H., Peng, P., and Spiro, B. (2016). Seasonal variability in concentrations and fluxes of glycerol dialkyl glycerol tetraethers in Huguangyan Maar Lake, SE China: implications for the applicability of the MBT–CBT paleotemperature proxy in lacustrine settings. *Chem. Geol.* 420, 200–212. doi:10.1016/j.chemgeo.2015.11.008

Huguet, A., Coffinet, S., Roussel, A., Gayraud, F., Anquetil, C., Bergonzini, L., et al. (2019). Evaluation of 3-hydroxy fatty acids as a pH and temperature proxy in soils from temperate and tropical altitudinal gradients. *Org. Geochem.* 129, 1–13. doi:10.1016/j.orggeochem.2019.01.002

Kou, Q., Zhu, L., Ju, J., Wang, J., Xu, T., Li, C., et al. (2022). Influence of salinity on glycerol dialkyl glycerol tetraether-based indicators in Tibetan Plateau lakes: implications for paleotemperature and paleosalinity reconstructions. *Palaeogeogr. Palaeoclimatol. Palaeoecol.* 601, 111127. doi:10.1016/j.palaeo.2022.111127

Lei, Y., Strong, D. J., Caballero, M., Correa-Metrio, A., Pérez, L., Schwalb, A., et al. (2023). Regional vs. global temperature calibrations for lacustrine BrGDGTs in the North American (sub)tropics: implications for their application in paleotemperature reconstructions. *Org. Geochem.* 184, 104660. doi:10.1016/j.orggeochem.2023.104660

Lei, Y., Yang, H., Dang, X., Zhao, S., and Xie, S. (2016). Absence of a significant bias towards summer temperature in branched tetraether-based paleothermometer at two soil sites with contrasting temperature seasonality. *Org. Geochem.* 94, 83–94. doi:10.1016/j.orggeochem.2016.02.003

Li, J., Naafs, B. D. A., Pancost, R. D., Yang, H., Liu, D., and Xie, S. (2017). Distribution of branched tetraether lipids in ponds from Inner Mongolia, NE China: insight into the source of brGDGTs. *Org. Geochem.* 112, 127–136. doi:10.1016/j.orggeochem.2017.07.005

Loomis, S. E., Russell, J. M., Heureux, A. M., D'Andrea, W. J., and Sinninghe Damsté, J. S. (2014). Seasonal variability of branched glycerol dialkyl glycerol tetraethers (brGDGTs) in a temperate lake system. *Geochimica Cosmochimica Acta* 144, 173–187. doi:10.1016/j.gca.2014.08.027

Loomis, S. E., Russell, J. M., Ladd, B., Street-Perrott, F. A., and Sinninghe Damsté, J. S. (2012). Calibration and application of the branched GDGT temperature proxy on East African lake sediments. *Earth Planet. Sci. Lett.* 357–358, 277–288. doi:10.1016/j.epsl.2012.09.031

Martin, C., Ménot, G., Thouveny, N., Davtian, N., Andrieu-Ponel, V., Reille, M., et al. (2019). Impact of human activities and vegetation changes on the tetraether sources in Lake St Front (Massif Central, France). *Org. Geochem.* 135, 38–52. doi:10.1016/j.orggeochem.2019.06.005

Martínez-Sosa, P., Tierney, J. E., Stefanescu, I. C., Dearing Crampton-Flood, E., Shuman, B. N., and Routson, C. (2021). A global Bayesian temperature calibration for lacustrine brGDGTs. *Geochimica Cosmochimica Acta* 305, 87–105. doi:10.1016/j.gca.2021.04.038

Miller, D. R., Habicht, M. H., Keisling, B. A., Castañeda, I. S., and Bradley, R. S. (2018). A 900-year New England temperature reconstruction from *in situ* seasonally produced branched glycerol dialkyl glycerol tetraethers (brGDGTs). *Clim. Past.* 14, 1653–1667. doi:10.5194/cp-14-1653-2018

Ning, D., Zhang, E., Shulmeister, J., Chang, J., Sun, W., and Ni, Z. (2019). Holocene mean annual air temperature (MAAT) reconstruction based on branched glycerol dialkyl glycerol tetraethers from Lake Ximenglongtan, southwestern China. *Org. Geochem.* 133, 65–76. doi:10.1016/j.orggeochem.2019.05.003

O'Beirne, M. D., Scott, W. P., and Werne, J. P. (2023). A critical assessment of lacustrine branched glycerol dialkyl glycerol tetraether (brGDGT) temperature calibration models. *Geochimica Cosmochimica Acta* 359, 100–118. doi:10.1016/j.gca.2023.08.019

Patil, I. (2021). Visualizations with statistical details: the 'ggstatsplot' approach. *J. Open Source Softw.* 6 (61), 3167. doi:10.21105/joss.03167

Pearson, E. J., Juggins, S., Talbot, H. M., Weckström, J., Rosén, P., Ryves, D. B., et al. (2011). A lacustrine GDGT-temperature calibration from the Scandinavian Arctic to Antarctic: renewed potential for the application of GDGT-paleothermometry in lakes. *Geochimica Cosmochimica Acta* 75, 6225–6238. doi:10.1016/j.gca.2011.07.042

Peterse, F., Vonk, J. E., Holmes, R. M., Giosan, L., Zimov, N., and Eglinton, T. I. (2014). Branched glycerol dialkyl glycerol tetraethers in Arctic lake sediments: sources and implications for paleothermometry at high latitudes: branched GDGTs in Arctic lakes. *J. Geophys. Res. Biogeosci.* 119, 1738–1754. doi:10.1002/2014jg002639

Powers, L. A., Werne, J. P., Johnson, T. C., Hopmans, E. C., Sinninghe Damsté, J. S., and Schouten, S. (2004). Crenarchaeotal membrane lipids in lake sediments: a new paleotemperature proxy for continental paleoclimate reconstruction? *Geol* 32, 613. doi:10.1130/g20434.1

Qian, S., Yang, H., Dong, C., Wang, Y., Wu, J., Pei, H., et al. (2019). Rapid response of fossil tetraether lipids in lake sediments to seasonal environmental variables in a shallow lake in central China: implications for the use of tetraether-based proxies. *Org. Geochem.* 128, 108–121. doi:10.1016/j.orggeochem.2018.12.007

Raberg, J. H., Flores, E., Crump, S. E., de Wet, G., Dildar, N., Miller, G. H., et al. (2022). Intact polar brGDGTs in arctic lake catchments: implications for lipid sources and paleoclimate applications. *JGR Biogeosciences* 127, e2022JG006969. doi:10.1029/2022jg006969

Raberg, J. H., Harning, D. J., Crump, S. E., de Wet, G., Blumm, A., Kopf, S., et al. (2021). Revised fractional abundances and warm-season temperatures substantially improve brGDGT calibrations in lake sediments. *Biogeosciences* 18, 3579–3603. doi:10.5194/bg-18-3579-2021

Russell, J. M., Hopmans, E. C., Loomis, S. E., Liang, J., and Sinninghe Damsté, J. S. (2018). Distributions of 5- and 6-methyl branched glycerol dialkyl glycerol tetraethers (brGDGTs) in East African lake sediment: effects of temperature, pH, and new lacustrine paleotemperature calibrations. *Org. Geochem.* 117, 56–69. doi:10.1016/j.orggeochem.2017.12.003

Russell, J. M., and Werne, J. P. (2007). The use of solid phase extraction columns in fatty acid purification. *Org. Geochem.* 38, 48–51. doi:10.1016/j.orggeochem.2006.09.003

Schouten, S., Hopmans, E. C., and Sinninghe Damsté, J. S. (2013). The organic geochemistry of glycerol dialkyl glycerol tetraether lipids: a review. *Org. Geochem.* 54, 19–61. doi:10.1016/j.orggeochem.2012.09.006

Sinninghe Damsté, J. S. S., Hopmans, E. C., Pancost, R. D., Schouten, S., and Geenevasen, J. A. J. (2000). Newly discovered non-isoprenoid glycerol dialkyl glycerol tetraether lipids in sediments. *Chem. Commun.*, 1683–1684. doi:10.1039/b004517i

Stefanescu, I. C., Shuman, B. N., and Tierney, J. E. (2021). Temperature and water depth effects on brGDGT distributions in sub-alpine lakes of mid-latitude North America. *Org. Geochem.* 152, 104174. doi:10.1016/j.orggeochem.2020.104174

Sun, Q., Chu, G., Liu, M., Xie, M., Li, S., Ling, Y., et al. (2011). Distributions and temperature dependence of branched glycerol dialkyl glycerol tetraethers in recent lacustrine sediments from China and Nepal. *J. Geophys. Res.* 116, G01008. doi:10.1029/2010jg001365

Tierney, J. E., and Russell, J. M. (2009). Distributions of branched GDGTs in a tropical lake system: implications for lacustrine application of the MBT/CBT paleoproxy. *Org. Geochem.* 40, 1032–1036. doi:10.1016/j.orggeochem.2009.04.014

Tierney, J. E., Russell, J. M., Eggermont, H., Hopmans, E. C., Verschuren, D., and Sinninghe Damsté, J. S. (2010). Environmental controls on branched tetraether lipid distributions in tropical East African lake sediments. *Geochimica Cosmochimica Acta* 74, 4902–4918. doi:10.1016/j.gca.2010.06.002

Tierney, J. E., Schouten, S., Pitcher, A., Hopmans, E. C., and Sinninghe Damsté, J. S. (2012). Core and intact polar glycerol dialkyl glycerol tetraethers (GDGTs) in Sand Pond, Warwick, Rhode Island (USA): insights into the origin of lacustrine GDGTs. *Geochimica Cosmochimica Acta* 77, 561–581. doi:10.1016/j.gca.2011.10.018

Véquaud, P., Derenne, S., Anquetil, C., Collin, S., Poulenard, J., Sabatier, P., et al. (2021a). Influence of environmental parameters on the distribution of bacterial lipids in soils from the French Alps: implications for paleo-reconstructions. *Org. Geochem.* 153, 104194. doi:10.1016/j.orggeochem.2021.104194

Véquaud, P., Derenne, S., Thibault, A., Anquetil, C., Bonanomi, G., Collin, S., et al. (2021b). Development of global temperature and pH calibrations based on bacterial 3-hydroxy fatty acids in soils. *Biogeosciences* 18, 3937–3959. doi:10.5194/bg-18-3937-2021

Véquaud, P., Thibault, A., Derenne, S., Anquetil, C., Collin, S., Contreras, S., et al. (2022). FROG: a global machine-learning temperature calibration for branched GDGTs in soils and peats. *Geochimica Cosmochimica Acta* 318, 468–494. doi:10.1016/j.gca.2021.12.007

Wang, H., Chen, W., Zhao, H., Cao, Y., Hu, J., Zhao, Z., et al. (2023). Biomarker-based quantitative constraints on maximal soil-derived brGDGTs in modern lake sediments. *Earth Planet. Sci. Lett.* 602, 117947. doi:10.1016/j.epsl.2022.117947

Wang, H., Liu, W., He, Y., Zhou, A., Zhao, H., Liu, H., et al. (2021). Salinity-controlled isomerization of lacustrine brGDGTs impacts the associated M B T 5 M E ' terrestrial temperature index. *Geochimica Cosmochimica Acta* 305, 33–48. doi:10.1016/j.gca.2021.05.004

Wang, H., Liu, W., and Lu, H. (2016). Appraisal of branched glycerol dialkyl glycerol tetraether-based indices for North China. *Org. Geochem.* 98, 118–130. doi:10.1016/j.orggeochem.2016.05.013

Wang, H., Liu, W., Zhang, C. L., Wang, Z., Wang, J., Liu, Z., et al. (2012). Distribution of glycerol dialkyl glycerol tetraethers in surface sediments of Lake Qinghai and surrounding soil. *Org. Geochem.* 47, 78–87. doi:10.1016/j.orggeochem.2012.03.008

Weber, Y., De, J. C., Rijpstra, W. I. C., Hopmans, E. C., Stadnitskaia, A., Schubert, C. J., et al. (2015). Identification and carbon isotope composition of a novel branched GDGT isomer in lake sediments: evidence for lacustrine branched GDGT production. *Geochimica Cosmochimica Acta* 154, 118–129. doi:10.1016/j.gca.2015.01.032

Weber, Y., Sinninghe Damsté, J. S., Zopfi, J., De Jonge, C., Gilli, A., Schubert, C. J., et al. (2018). Redox-dependent niche differentiation provides evidence for multiple bacterial sources of glycerol tetraether lipids in lakes. *Proc. Natl. Acad. Sci. U.S.A.* 115, 10926–10931. doi:10.1073/pnas.1805186115

Weijers, J. W. H., Schouten, S., Hopmans, E. C., Geenevasen, J. A. J., David, O. R. P., Coleman, J. M., et al. (2006). Membrane lipids of mesophilic anaerobic bacteria thriving in peats have typical archaeal traits. *Environ. Microbiol.* 8, 648–657. doi:10.1111/j.1462-2920.2005.00941.x

Wickham, H. (2016). *ggplot2: Elegant Graphics for Data Analysis*. New York: Springer-Verlag. Available at: https://ggplot2.tidyverse.org.

Wu, J., Yang, H., Pancost, R. D., Naafs, B. D. A., Qian, S., Dang, X., et al. (2021). Variations in dissolved O2 in a Chinese lake drive changes in microbial communities and impact sedimentary GDGT distributions. *Chem. Geol.* 579, 120348. doi:10.1016/j.chemgeo.2021.120348

Xiao, W., Wang, Y., Zhou, S., Hu, L., Yang, H., and Xu, Y. (2016). Ubiquitous production of branched glycerol dialkyl glycerol tetraethers(brGDGTs) in global marine environments: a new source indicator for brGDGTs. *Biogeosciences* 13, 5883–5894. doi:10.5194/bg-13-5883-2016

Xiao, W., Xu, Y., Ding, S., Wang, Y., Zhang, X., Yang, H., et al. (2015). Global calibration of a novel, branched GDGT-based soil pH proxy. *Org. Geochem.* 89–90, 56–60. doi:10.1016/j.orggeochem.2015.10.005

Yamamoto, M., Shimamoto, A., Fukuhara, T., and Tanaka, Y. (2016). Source, settling and degradation of branched glycerol dialkyl glycerol tetraethers in the marine water column. *Geochimica Cosmochimica Acta* 191, 239–254. doi:10.1016/j.gca.2016.07.014

Yang, H., Lü, X., Ding, W., Lei, Y., Dang, X., and Xie, S. (2015). The 6-methyl branched tetraethers significantly affect the performance of the methylation index (MBT′) in soils from an altitudinal transect at Mount Shennongjia. *Org. Geochem.* 82, 42–53. doi:10.1016/j.orggeochem.2015.02.003

Yao, Y., Zhao, J., Vachula, R. S., Werne, J. P., Wu, J., Song, X., et al. (2020). Correlation between the ratio of 5-methyl hexamethylated to pentamethylated branched GDGTs (HP5) and water depth reflects redox variations in stratified lakes. *Org. Geochem.* 147, 104076. doi:10.1016/j.orggeochem.2020.104076

Zhang, C., Zhao, C., Zhou, A., Zhang, H., Liu, W., Feng, X., et al. (2021). Quantification of temperature and precipitation changes in northern China during the "5000-year" Chinese History. *Quat. Sci. Rev.* 255, 106819. doi:10.1016/j.quascirev.2021.106819

Zhao, B., Castañeda, I. S., Bradley, R. S., Salacup, J. M., de Wet, G. A., Daniels, W. C., et al. (2021). Development of an *in situ* branched GDGT calibration in Lake 578, southern Greenland. *Org. Geochem.* 152, 104168. doi:10.1016/j.orggeochem.2020.104168

Zhao, B., Russell, J. M., Tsai, V. C., Blaus, A., Parish, M. C., Liang, J., et al. (2023). Evaluating global temperature calibrations for lacustrine branched GDGTs: seasonal variability, paleoclimate implications, and future directions. *Quat. Sci. Rev.* 310, 108124. doi:10.1016/j.quascirev.2023.108124

Zink, K.-G., Vandergoes, M. J., Mangelsdorf, K., Dieffenbacher-Krall, A. C., and Schwark, L. (2010). Application of bacterial glycerol dialkyl glycerol tetraethers (GDGTs) to develop modern and past temperature estimates from New Zealand lakes. *Org. Geochem.* 41, 1060–1066. doi:10.1016/j.orggeochem.2010.03.004